Chapter 1

Introduction

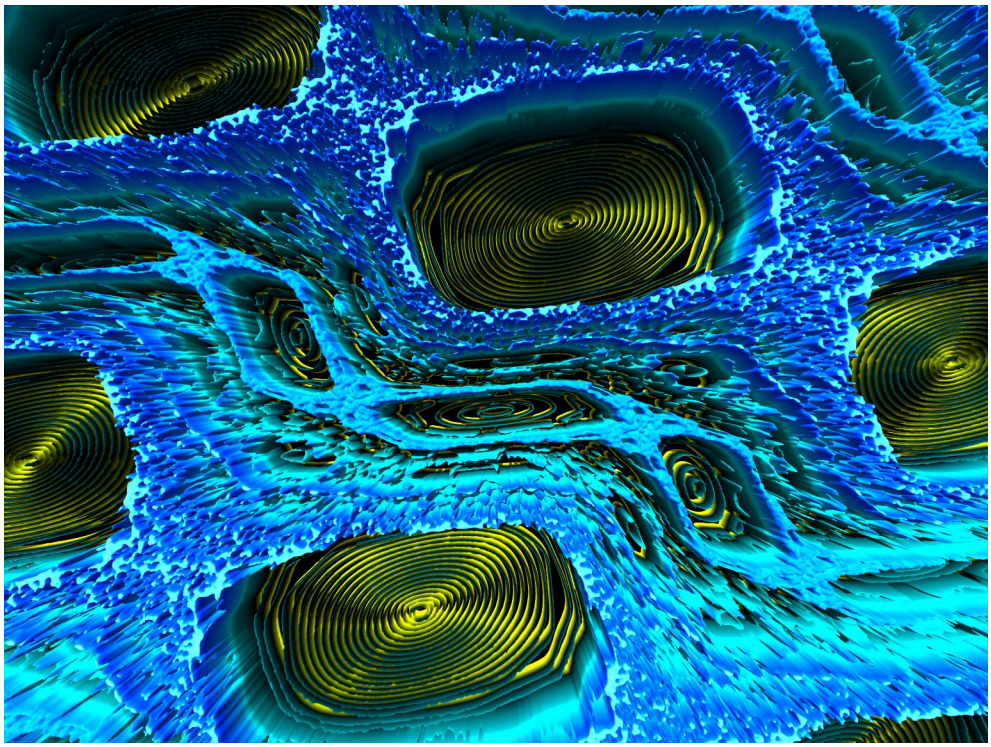

1.1 Classical Chaos

The study of chaos in dynamical systems originated near the end of the 19th century [Moser73; Moser78; Reichl92; Peterson93]. At the time, Newtonian mechanics gave an impressively accurate description of the motion of the bodies in the solar system, even prompting (somewhat serendipitously) the discovery of Neptune, in order to explain a discrepancy between the predicted and observed trajectories of Uranus. Although the problem of the dynamics of three gravitationally interacting bodies was not (and still is not) analytically solvable in general, much headway was made in the prediction of planetary locations by first considering only the interaction of each planet with the sun, and then taking into account the perturbations due to the interactions of the planets with each other. The apparent clock-like regularity of the solar system and the accuracy with which the planetary motion could be computed prompted the question of the stability of the solar system: would the solar system continue in its usual fashion, with the planets maintaining their regular orbits, or could the motion of the planets change drastically in the future? Showing that the solar system is indeed stable, which amounts to showing that successive corrections (perturbations) to the planetary motion converge, was at the time considered quite important. In fact, it was posed by Weierstrass, after a comment by Dirichlet, as one of the prize questions in a contest, organized by Mittag-Leffler, in honor of King Oscar II of Sweden and Norway. Henri Poincaré submitted a complex and innovative entry that demonstrated the stability in the three-body problem and was named the winning entry. However, after its publication it was pointed out that Poincaré had made a significant error in his proof. Mittag-Leffler's rather drastic response was to recall and destroy every copy of the issue of *Acta Mathematica* in which Poincaré's proof appeared. Poincaré subsequently produced a revised work that instead appeared as the prize-winning entry; however, this revised work contained the opposite conclusion: the stability of the solar system could not be guaranteed. The ideas embodied in this work prompted Poincaré's later famous statement of how minute differences in the initial conditions of a system can lead to wildly different outcomes. This is the key notion of chaotic dynamical systems, which has the consequence that small but inevitable errors in our knowledge of the state of a system necessarily forbid accurate, long-term predictions of the system's evolu-

tion. Thus, despite the deterministic nature of chaotic systems, their dynamics are inherently unpredictable, and they appear to be random.

Despite Poincaré's remarkable achievement, the study of chaos did not really take off for several decades, although there were several important results during this period by George Birkhoff and Carl Ludwig Siegel, among others. In the 1950's and 60's the problem of stability in the three-body problem was revisited, and an important result was obtained in stages by Andrei N. Kolmogorov, Vladimir I. Arnol'd, and Jürgen Moser, in the celebrated KAM theorem [Moser73; Moser78; Tabor89]. This result restored the stability of the solar system in the sense that it showed that certain configurations are stable while others were unstable (at least in restricted versions of the solar system). Furthermore, if the aforementioned perturbations are small, then most of the possible configurations are stable. So, although the stability of the solar system seems to be assured, this whole series of events resulted in the important recognition of the possibility of chaos.

The study of chaotic systems began in earnest with the advent of computers, which facilitated the study of the inherent complexity of chaotic systems. This line of study began with the work of Edward Lorenz, who found this same sort of instability in numerical "experiments" studying a hydrodynamic system, which served as a very basic model for the atmosphere [Lorenz63]. Since then, chaos has been found to be ubiquitous both in physics as well as in other disciplines, having found applications in such diverse phenomena as plasma confinement [Hazeltine92], laser dynamics [Roy92], chemical reactions [Simoyi82], cardiac rhythms [Glass86], and disease epidemiology [Schaffer86]. Chaos is also important in the study of dynamical systems, as chaos is the rule rather than the exception, despite the traditional textbook view of physics.

The term "chaos" was introduced [Li75] to refer to this "deterministic randomness" in dynamical systems. However, it is still difficult to provide a definition of chaos that is universally accepted. On the other hand, it is possible to point out some important characteristics of systems that we refer to as being chaotic:

1. As mentioned before, a *dynamical instability* leading to unpredictability is a central characteristic of chaos. Furthermore, this instability should be *exponential* rather than *linear* in time, since in the linear case predictability is possible even in the presence of a slight uncertainty if a sufficiently long history of the system is known. In the exponential (chaotic) case, however, no additional predictive power is gained by knowing the system history beyond the initial condition [Chirikov91]. These properties can be more formally quantified using the *Lyapunov exponent* and the *Kolmogorov-Sinai entropy* [Ott93; Lichtenberg92].

2. The instability is purely *deterministic* and intrinsic to the dynamics; the chaos is not explained by external noise [Chirikov91].

3. The instability should be *global* in the sense that chaotic behavior occurs for a range of conditions and is not limited to a set of zero measure in phase space (defined below), as in the unstable configuration of a perfectly inverted pendulum. Also, the chaotic trajectories should be *ergodic*, so that they eventually wander throughout the possible range of chaotic trajectories (although it is possible to find disconnected regions of chaos in weakly perturbed Hamiltonian systems, as we briefly discuss below, and in dissipative systems, the trajectories are only ergodic over the "attracting set").

4. The system should be in some sense *bounded*, to avoid trivial exponential separation of trajectories, as in $x(t) = x_0 \exp(t)$ for different x_0. To keep the trajectories confined as they separate from each other, there must be some notion of "stretching and folding," as exemplified in the Smale horseshoe map [Hilborn94]. Another related property is that each point on a chaotic trajectory should lie arbitrarily close to a periodic trajectory (i.e., a trajectory that repeats itself in finite time) [Devaney89].

5. The physical model of the system should be *simple*. It is surprising that simple systems such as the three-body problem can give rise to such complicated and unpredictable behavior, but complicated behavior is *not* surprising in a system with many degrees of freedom. So, for example, although Brownian motion is unpredictable, a deterministic physical model would include the collisional interactions of a macroscopic number of gas

molecules; hence, we would not call this system chaotic. (Note that there are methods for analyzing data to distinguish low-dimensional chaos from such high-dimensional noise [Sugihara90; Tsonis92].)

When we return to the concept of integrability below, we can be more precise about the meaning of chaos, at least in Hamiltonian systems.

As an example of the distinction between determinism and predictability in chaotic systems, consider the *standard map*, which models one of the two classically chaotic systems presented in this dissertation. The standard map is a set of two equations,

$$\begin{aligned} p_{n+1} &= p_n + K \sin x_n \\ x_{n+1} &= x_n + p_{n+1} \quad , \end{aligned} \tag{1.1}$$

where the sole parameter K controls the "degree of chaos" of the map. This mapping is iterated to determine a *trajectory* (x_0, p_0), (x_1, p_1), ..., (x_n, p_n). These equations are, of course, deterministic, in that there is no random element involved. In fact, though this map looks quite simple, it gives rise to rich and complicated dynamics. The characteristic lack of predictability in this map is illustrated in Fig. 1.1, where the standard map is iterated with the same initial condition on four different computers. Even though the results should be identical among the four computers, they only agree for around 16 iterations. Beyond this point the trajectories diverge, and prediction clearly becomes meaningless. In principle, it is possible to make meaningful predictions over a larger number of iterations by using greater precision in the computations. However, a *linear* increase in prediction time requires an *exponential* increase in the numerical precision. More importantly, for modeling physical systems, the precision with which the initial state of the system is known nearly always limits the prediction time.

Despite this lack of predictability, chaotic systems can still be meaningfully studied. The unpredictability that we have indicated thus far is for a trajectory evolving from a particular initial state. The numerically generated trajectory, referred to as a *pseudotrajectory*, diverges away from the real trajectory with the same initial condition; however, it is often possible to find another real trajectory with a slightly different initial condition that *shadows* the pseudotrajectory in the sense that it remains close to the pseudotrajectory for long times. This shadowing

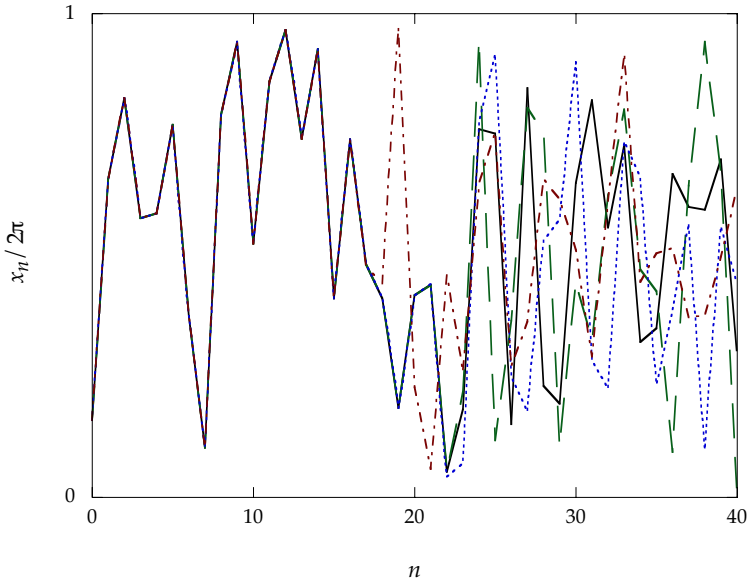

Figure 1.1: Numerical iteration of the standard map, illustrating the inherently unpredictable nature of chaotic systems. The same FORTRAN77 code was executed on four modern computers to iterate the standard map for $K = 10$ and the initial condition $(x_0, p_0) = (1, 1)$. The spatial coordinate x_n (taken modulo 2π) is plotted for the first 40 iterations of the standard map. Although nominally the same (64-bit, or around 15-digit) "double precision" numerical representation was used on the different computers, slight differences in the numerical rounding methods among the processors are rapidly amplified as the iterations progress. Hence, the trajectories are identical only for the first few iterations, and they become completely uncorrelated after about 25 iterations. The processors employed here were a Motorola PowerPC 750 (solid line), an Intel Pentium III (dashed line), a MIPS/SGI R10000 (dotted line), and a Cray SV1 processor (dash-dotted line).

occurs for arbitrarily long times in a restricted class of systems ("hyperbolic systems," which are comparatively rare), but shadowing occurs also for generic (nonhyperbolic) chaotic systems for long times between "glitches" [Grebogi90; Sauer91; Sauer97]. An important consequence of this effect is that *global* or *statistical* predictions regarding ensembles of trajectories are still meaningful and can be accurately computed, implying a *robustness* or *structural stability* under sufficiently small perturbations [Chirikov91]. So, the study of chaotic systems involves a shift to asking different kinds of questions, and in this way much progress has been made in uncovering universal structure and behavior in chaotic systems. This notion was recognized early on by Poincaré, who developed a geometric approach to studying dynamical systems that we introduce in the next section.

1.1.1 Phase Space

Now we explore the concept of *phase space*, whose graphical depiction, the *phase portrait*, is a powerful tool for visualizing the behavior of dynamical systems. The phase space of a dynamical system is the space of points that completely specify the state of the system. In a coordinate representation, a dynamical system can be expressed as a set of first-order differential equations:

$$\begin{aligned} \partial_t x_1 &= f_1(x_1, x_2, \ldots, x_n) \\ \partial_t x_2 &= f_2(x_1, x_2, \ldots, x_n) \\ &\vdots \\ \partial_t x_n &= f_n(x_1, x_2, \ldots, x_n) \end{aligned} \tag{1.2}$$

(where $\partial_t \equiv \partial/\partial t$). This dynamical system is *autonomous*, since the f_i do not explicitly depend on time, but an external periodic drive can be accounted for by introducing time as an auxiliary coordinate [Ott93]. Then the phase space for this system is the set of all n-tuples $(x_1, x_2, \ldots, x_n)$. The location in phase space at a particular time together with the model functions f_i then completely specify the state of the system for all values of the time parameter t.

In this work we are interested in *Hamiltonian systems*. These systems are characterized by a Hamiltonian function $H(x_i, p_i, t)$, such that the dynamics in terms of the "canonical coordinates" x_i and p_i are given by Hamilton's equations:

$$\begin{aligned} \partial_t x_i &= \partial_{p_i} H \\ \partial_t p_i &= -\partial_{x_i} H \quad . \end{aligned} \tag{1.3}$$

The phase space is then simply the space of the canonical positions x_i and momenta p_i. In the special case where the Hamiltonian is independent of time, the system is said to be *conservative* in that the energy (the particular value of H for a given phase-space point) is a conserved quantity, which follows directly from Eqs. (1.3). For time-dependent Hamiltonian systems, the energy is not conserved, but all Hamiltonian systems are characterized by the more general conservation property that volumes in phase space are preserved under time evolution as a consequence of Liouville's theorem (and as a special case of Poincaré's integral invariants) [Tabor89].

The simplest Hamiltonian systems that one can consider are of one dimension (or one *degree of freedom*) and time-independent, where the two-dimensional phase space is spanned

by the pair of variables (x, p). The trajectories in this phase space are simply the surfaces of constant energy, because energy is a conserved quantity. We illustrate such a phase space by considering the pendulum, where the Hamiltonian is

$$H(x,p) = \frac{p^2}{2} - \cos x \quad . \tag{1.4}$$

The phase portrait for the pendulum is shown in Fig. 1.2. There are several interesting features to note in the phase portrait. One type of motion, known as "libration" (or "oscillation"), appears as a set of elliptical contours, along which the trajectories flow in the clockwise direction. These trajectories correspond to the pendulum motion one observes in the operation of a grandfather

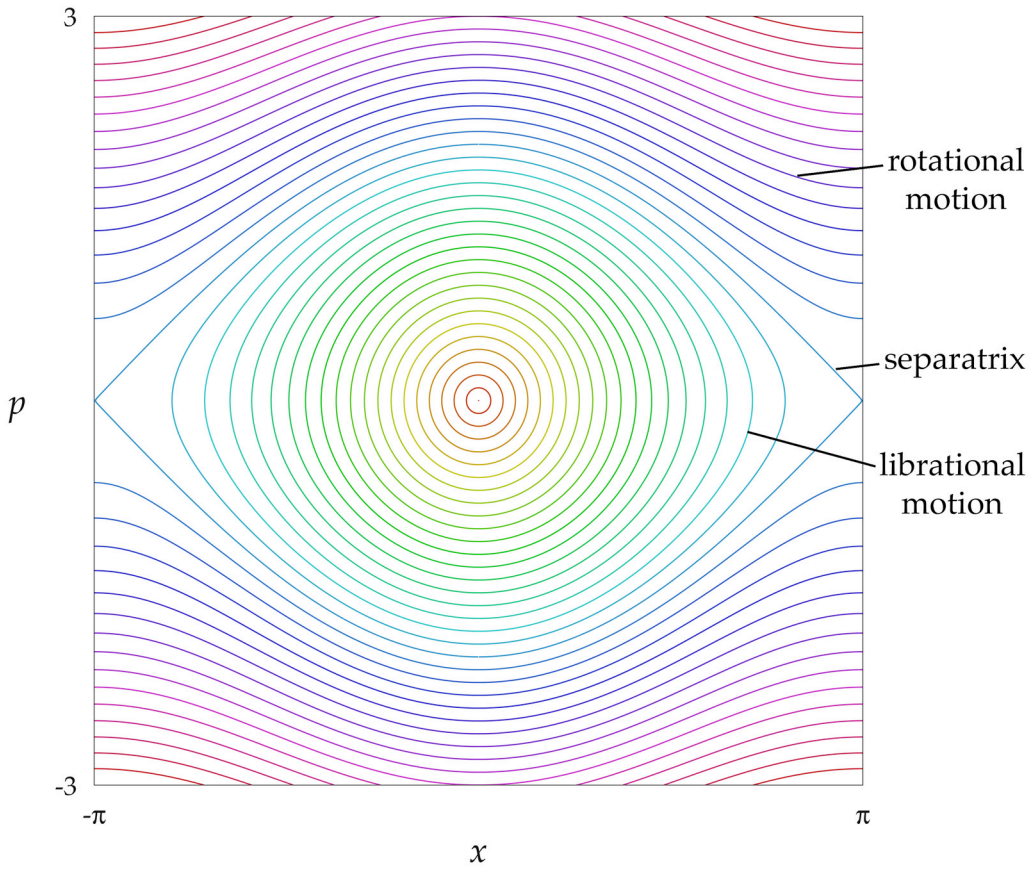

Figure 1.2: Plot of the phase space for the pendulum. The curves (trajectories) are the level sets of the pendulum Hamiltonian, Eq. (1.4). The different colors correspond to trajectories beginning from different initial conditions.

clock, and they emanate from a stable *fixed point* at $(x, p) = (0, 0)$, which corresponds to the resting configuration of the pendulum. Another fixed point occurs at $(x, p) = (\pi, 0)$ (which is equivalent to the point $(-\pi, 0)$ because of the spatial periodicity of the Hamiltonian), and describes the stationary but unstable configuration of an inverted pendulum. Another distinct type of motion is "rotation," which appears as a set of curves that do not cross the $p = 0$ axis. For this motion the trajectories flow to the right in the upper half-plane and to the left in the lower half-plane. These trajectories correspond to more rapid motion of the pendulum such that the pendulum does not reverse direction as in the librational case, but rather continues "over the top." The boundary between the two types of motion is the *separatrix*, which passes through the unstable fixed point. From this example, we can see that the phase portrait gives a concise, visual summary of the possible dynamics of a system (although the time-dependence of the trajectories must still be extracted from the equations of motion).

In the experiments described later on, we study time-periodic ("driven"), one-dimensional Hamiltonian systems. In this case, the phase space is of higher dimension than in the time-independent case, since time acts as an effective extra dimension. In fact, it can be shown that these systems (referred to as $1\frac{1}{2}$-degree-of-freedom systems) are formally equivalent to two-degree-of-freedom systems [Morrison96]. So, the flow of these systems cannot be represented in a planar plot in the same way as one-dimensional systems. However, one can instead use a reduced phase plot, known as a *Poincaré surface of section*, which is a plane of constant t, modulo the period of the external drive. The plot constructed in this way consists of the intersections of the trajectories with the surface of section, which appear as dots in the plane, each corresponding to the coordinates (x, p) plotted once per drive period. This phase portrait still captures the full dynamics, since each point in the phase plot uniquely determines all the successive points in the trajectory. Sample phase portraits of this type are shown in Fig. 1.3, for the pendulum with a weak, sinusoidal amplitude modulation, and in Fig. 1.4, for a strongly amplitude-modulated pendulum, corresponding to the system studied in much greater detail in Chapter 6. This surface-of-section technique also works for two-dimensional autonomous systems, which have four coordinates in the full phase space, since the conserved energy eliminates

one of the coordinates, and the phase plane is taken to be at a constant value of another of the coordinates (where the intersections are also usually only plotted for one direction of passage through the surface). This technique can be used to study systems with more than two degrees of freedom, but then the location in the phase plane no longer uniquely determines the rest of the trajectory.

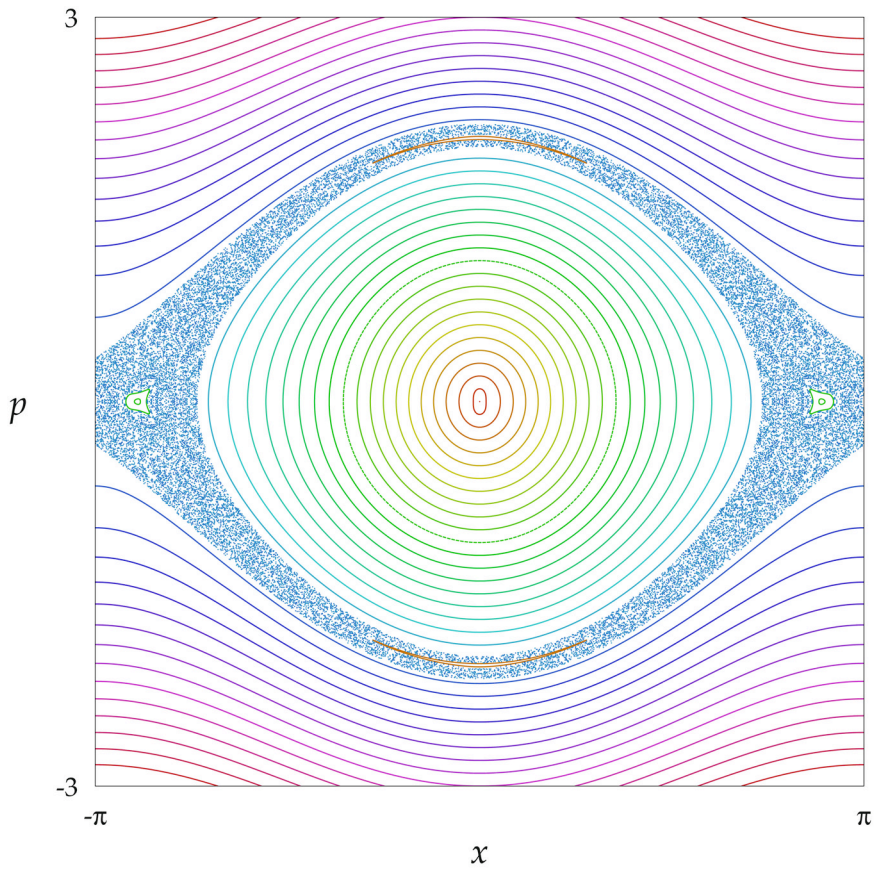

Figure 1.3: Phase space (Poincaré section) of a pendulum with a weak amplitude drive, with Hamiltonian $H = p^2/2 - (1 + 0.05\cos t)\cos x$. This "stroboscopic" plot is sampled at every $t = 2\pi n$ for integer n. As expected from KAM theory, most of the stable structure of the pendulum is left unchanged by the weak drive. However, the separatrix has broken down into a disordered region of chaos.

1.1.2 Integrability and Chaos

Now we will specialize our discussion of chaos to Hamiltonian systems, which will be our main interest in this work. Before doing so, however, we note that nonlinearity is an essential ingredient for producing chaotic behavior. Returning to the general dynamical system described by Eqs. (1.2), if this system is linear, then the equations can be expressed in terms of a matrix as

$$\partial_t x_i = \sum_j M_{ij}\, x_j \quad . \tag{1.5}$$

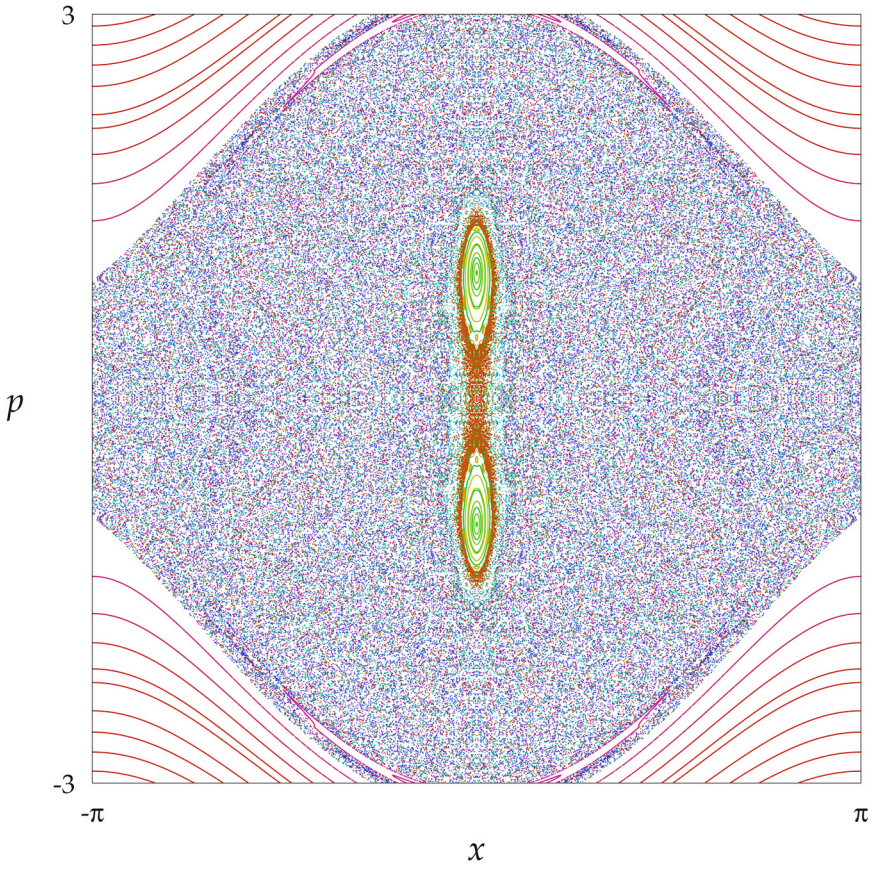

Figure 1.4: Phase space (Poincaré section) of a pendulum with a strong amplitude drive, with Hamiltonian $H = p^2/2 - (1 + \cos t)\cos x$. The stronger modulation here, compared to Fig. 1.3, breaks down most of the stable pendulum structure, resulting in widespread chaos.

This linear system of equations then has the solution [Mirsky90]

$$x_i(t) = \sum_j \exp(\mathbf{M}t)_{ij}\, x_j(0) \quad , \tag{1.6}$$

where $\exp(\mathbf{A})$ is the matrix exponential of the square matrix $\mathbf{A}$, which is defined in terms of the usual Taylor series expansion of the exponential function and exists for any matrix. Hence, linear systems are quasiperiodic (i.e., having a discrete frequency spectrum) in steady state and therefore predictable; by contrast, chaotic systems are characterized by continuous power spectra [Ott93; Chirikov91].

Turning back now to Hamiltonian systems, we can see that no chaos occurs in one-dimensional autonomous Hamiltonian systems, because the existence of a conserved quantity, the energy $E(x,p)$, allows for the solution [Morrison96]

$$t = \int_{x(0)}^{x} dx' \, [\partial_p H(x',p)]^{-1} \quad , \tag{1.7}$$

where p is regarded as a function of x and E. This solution must then be inverted to obtain $x(t)$ (and hence $p(t)$). So, the phase-space trajectories are regular for all one-dimensional autonomous Hamiltonians, as is the case for the pendulum example in Fig. 1.2 (indeed, any continuous dynamical system of the form of Eqs. (1.2) with $n = 2$ is free of chaotic behavior [Ott93]). As a result, Hamiltonian systems of one degree of freedom are said to be *integrable*.

The important point of integrability in one dimension is the existence of a constant of the motion. In the case of N degrees of freedom, the system is integrable if there exist N independent constants of the motion I_k that are *in involution*, which means that their Poisson brackets (taken pairwise) vanish:

$$\{I_j, I_k\}_{\mathrm{P}} := \sum_{i=1}^{N} [(\partial_{x_i} I_j)(\partial_{p_i} I_k) - (\partial_{p_i} I_j)(\partial_{x_i} I_k)] = 0 \quad (\forall\, j,k \in \{1,\ldots,N\}) \quad . \tag{1.8}$$

These constants of the motion are related by Noether's theorem [Reichl92] to symmetries of the system (in the one-dimensional case, the constance of the energy is a consequence of the time-invariance of the Hamiltonian). The existence of these constants insures that the motion of trajectories in the $2N$-dimensional phase space is restricted to N-dimensional surfaces; under

slightly more restrictive assumptions, these surfaces are N-tori, and there exists a canonical transformation to *action-angle* coordinates, in which the dynamics are similar to that of a free particle (and hence not chaotic) [Morrison98]. *Separable* systems, where the Hamiltonian has the form

$$H(x_1, \ldots, x_N, p_1, \ldots, p_N) = H_1(x_1, p_1) + \cdots + H_N(x_N, p_N) \ , \tag{1.9}$$

form a special class of higher-dimensional, integrable systems. These systems are clearly integrable, because they are composed of uncoupled one-dimensional systems.

Generic Hamiltonian systems do not possess the high degree of symmetry required for integrability. In the case of the $1\frac{1}{2}$-degree-of-freedom systems studied in this work, the external periodic drive breaks the time-invariance of the Hamiltonian and thus opens up the possibility for chaotic behavior. When discussing the formation of chaos in Hamiltonian systems, it is common to start with an integrable system (such as the pendulum in Fig. 1.2) and view the symmetry-breaking interaction as a perturbation. When a weak perturbation is added, as in Fig. 1.3, *nonlinear resonances* between the degrees of freedom can occur. By the Poincaré–Birkhoff fixed-point theorem [Tabor89], these resonances produce pendulum-like structures in the phase space (for weak perturbations). In Fig. 1.3, several nonlinear resonances are apparent, including the original structure of the unperturbed pendulum around the stable fixed point as well as two other pairs of resonances (although arbitrarily many more are present on smaller scales). Note that the corresponding structure in the unperturbed pendulum is not in itself a nonlinear resonance, though, because it is not the direct result of coupling between two degrees of freedom. Although a single (isolated) resonance does not result in chaotic behavior [Walker69], the presence of multiple resonances causes their separatrices to broaden into chaotic regions [Chirikov79] (or homoclinic "tangles" [Ozorio de Almeida88; Tabor89]), as is shown by the diffuse area around the central resonance in Fig. 1.3. Picturesquely, these resonances are referred to as "islands of stability in a sea of chaos."

As expected from KAM theory, the weak perturbation in Fig. 1.3 leaves most of the stable structure intact. The invariant surfaces that survive the perturbation are thus referred to as "KAM surfaces." For the much stronger perturbation in Fig. 1.4, most of the stable structure has

degenerated into chaos. The chaotic region in this system is bounded in momentum, though, because for sufficiently large momentum the kinetic energy dominates the perturbing interaction, restoring stability. The chaotic motion due to the interaction of the resonances can be thought of as competition between different stable motions, where the trajectory is not dominated by any one of the motions (as is the case for trajectories in an island of stability).

1.2 Quantum Chaos

The field of quantum chaos, which brings together the study of classical chaotic dynamics and quantum-mechanical systems, is a relatively new area of study, especially considering how long the fundamental ideas of its two parent fields have been around. Interestingly, the first notions of quantum chaos seem to have predated quantum mechanics itself: the problem of "Chladni figures," the patterns of dust formed on thin, rigid, vibrating plates, was understood in the 19th century for plates with simple shapes, but not for plates with irregular borders [Stöckmann99]. (Actually, this problem belongs to a more general class of "wave chaos" problems, but as in microwave cavities and surface waves in fluids, these systems are equivalent to quantum "billiard" systems in the sense of time-independent quantum mechanics [Stöckmann99].) Einstein [Einstein17] realized as early as 1917 that there could be problems quantizing classical systems in the "old" quantum theory, where the classical tori with actions given by a multiple of Planck's constant $\hbar$ were associated with quantum states (according to the Bohr-Sommerfeld and later the Einstein-Brillouin-Keller quantization rules) [Tabor89; Brack97; Zaslavsky81]. This quantization procedure, while emphasizing the connection with the underlying classical description, obviously fails for chaotic systems where action-angle variables do not exist. The advent of the "new" (Schrödinger/Heisenberg) quantum mechanics effectively sidestepped these problems by creating a very different formalism, and it was not until much later that these ideas were once again appreciated [Tabor89]. Indeed, most of the progress in the field of quantum chaos has been made only during the last quarter century.

As in classical Hamiltonian systems, there is a sense of integrability in quantum systems. Symmetries also lead to conserved quantities in quantum mechanics in the form of quantum

numbers, which are the eigenvalues of operators that "generate" the transformation under which the system is invariant. For an N-dimensional quantum problem, if there are N operators $\hat{I}_k$ associated with conserved quantities that pairwise commute,

$$[\hat{I}_j, \hat{I}_k] := \hat{I}_j \hat{I}_k - \hat{I}_k \hat{I}_j = 0 \ \ (\forall\, j,k \in \{1,\ldots,N\}) \ \ , \tag{1.10}$$

the N ("simultaneous") operator eigenvalues completely specify the state of the system as well as its time evolution [Eckhardt88; Reichl92]. This requirement on the quantum operators is formally analogous to the classical definition of integrability, since the existence of N constants in involution as in Eq. (1.8) implies the existence of N vector fields,

$$L_{I_k} = \sum_{i=1}^{N} (\partial_{p_i} H)\partial_{q_i} - (\partial_{q_i} H)\partial_{p_i} \tag{1.11}$$

(such that the flow of the trajectories along the L_{I_k} leaves I_k unchanged), that pairwise commute [Eckhardt88; Morrison96]:

$$[L_{I_j}, L_{I_k}] = 0 \ \ (\forall\, j,k \in \{1,\ldots,N\}) \ \ . \tag{1.12}$$

Alternatively, the pairwise vanishing of the classical constants in the Poisson bracket carries over more directly to the quantum case in the form of the Moyal bracket [Eckhardt88; Reichl92], defined in Section 1.3.2 below. In any case, quantum "nonintegrability" occurs when symmetries are broken, leading to the loss of "good" (conserved) quantum numbers.

Because classical nonintegrability leads to chaotic behavior, one might expect something similar to happen for quantum nonintegrable systems. Surprisingly, though, classical chaos is suppressed in quantum systems. This was discovered numerically in a seminal study by Casati, Chirikov, Izrailev, and Ford (CCIF) [Casati79] of the quantum version of the standard map (1.1), obtained by quantizing the kicked-rotor Hamiltonian,

$$H = \frac{p^2}{2} + K\cos x \sum_n \delta(t-n) \ \ , \tag{1.13}$$

which generates the classical standard map. (We will treat this problem in detail in Chapter 4.) CCIF studied the kicked rotor in the regime where the phase space is characterized

by widespread chaos. The classical signature of chaos here is diffusion of an ensemble of trajectories in momentum as they gain energy, on average, from the time-dependent potential. Quantum mechanically, though, CCIF found that the kicked rotor gains energy as in the classical case only for a short time, after which the diffusion is suppressed. This effect has come to be known as *dynamical localization*, and is a dramatic example of how quantum effects suppress classical chaos. Shepelyansky [Shepelyansky83] has also provided a striking numerical demonstration of the suppression of chaos in the quantum kicked rotor, as we illustrate in Fig. 1.5. In this simulation, the classical and quantum systems evolve for some time from the same initial condition, and the suppression of energy growth by dynamical localization is evident in the quantum case. After evolving for some duration, a time-reversal is performed. In principle, both models should reverse their behavior and return to their initial conditions. The classical system only successfully contracts for a short time, though, and due to the buildup of numerical roundoff errors, the trajectories "forget" their history and the ensemble resumes diffusion, as expected for chaotic dynamics. The quantum system, on the other hand, makes a clean return to the initial state, indicating a robustness against perturbations and thus an absence of chaos. Note that such stability is expected in bounded quantum-mechanical systems, since they must have discrete spectra and thus exhibit almost-periodic dynamics [Hogg82].

1.2.1 Quantum Chaology

The apparent irony, then, of the field of quantum chaos is that it is the study of that which does not exist. Nonetheless, there are still some manifestations of the underlying classical disorder. One of the best-known examples is the disorder of the energy-levels in quantum nonintegrable systems, where the energy-level statistics are equivalent to those of random-matrix eigenvalues [McDonald79; Bohigas84; Tabor89; Reichl92]. Although the disorder in the spectra reflects the underlying (classical) dynamical disorder, this disorder is not unpredictable in the sense of dynamical chaos, because the spectral features can be computed with high accuracy [Delande01]. The quantum-localization effect that we already discussed is another manifestation of the classical chaos. It has been shown [Fishman82; Grempel84] that the kicked rotor can be mapped onto the Anderson localization problem [Anderson58], where a particle is spatially localized by

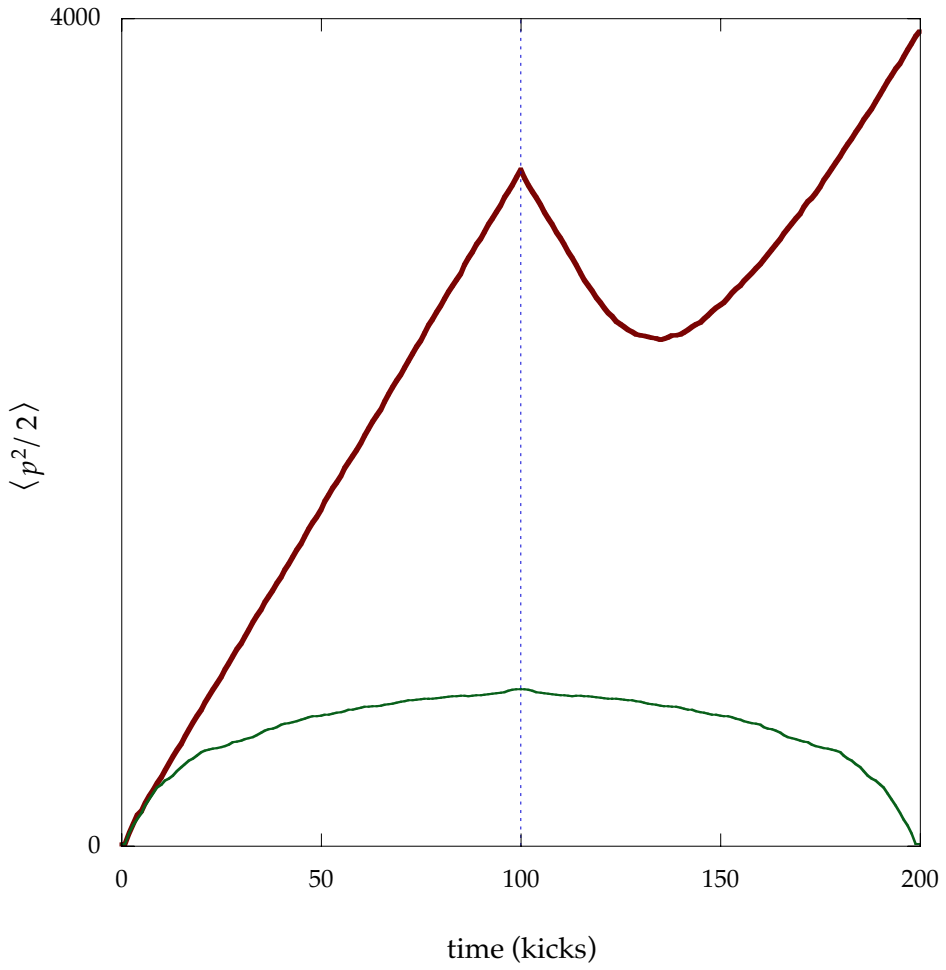

Figure 1.5: Comparison of classical (heavy solid line) and quantum (thin solid line) momentum transport in the kicked rotor for $K = 10$ and scaled Planck constant $\bar{k} = 1$ (simulation). The quantum initial condition is a Gaussian (minimum-uncertainty) wave packet with $\sigma_p = 2.5$, and the kinetic energy $\langle p^2/2 \rangle$ is plotted as a function of time; the classical evolution is the corresponding average for an ensemble of initial points picked according to the quantum distribution. The classical transport is diffusive, as characterized by the linear growth of energy. The quantum transport only shows diffusion for short times, and displays localization for longer times. At 100 kicks (marked by the dashed line), the direction of time is reversed. The classical ensemble resumes diffusive behavior after numerical errors build up in the simulation (thus converting the "special" trajectories that evolve back to the initial condition into generic, diffusing trajectories), which is typical for chaotic dynamics. The quantum system, on the other hand, retraces its steps back to its initial condition with high fidelity, indicating a lack of chaos. Note that in this quantum calculation, x is treated as an extended coordinate (as is the case in the experiment), necessitating a large (2×10^6 points) numerical grid to avoid aliasing effects.

the influence of a disordered potential. Thus in dynamical localization, the disorder that causes energy localization is not truly random (in the sense of an externally imposed randomness), but is generated dynamically by the underlying classical chaos. The chaos-assisted tunneling effect that we discuss in Chapter 6 also reflects the disorder associated with the classical chaos. Since the tunneling rate is strongly influenced by the states inside the chaotic sea, and these states are very sensitive to changes in the system parameters, the tunneling rate shows strong fluctuations as a parameter varies. Similar fluctuations are also apparent, for example, in the conduction of mesoscopic semiconductor structures [Marcus92; Stöckmann99], but it is worth reiterating that these symptoms of disorder are not chaotic in the classical sense.

In light of this suppression of chaos in quantum systems, Berry has introduced the term *quantum chaology* [Berry87; Berry91] to refer to the study of the "fingerprints" or "signatures" of classical chaos in their quantized counterparts (of which the above phenomena are examples, as well as the "scarring" of eigenstates along unstable periodic orbits [Heller84]). This is precisely the approach to quantum chaos adopted in this work, as we embark on a detailed investigation of localization, tunneling, and other quantum transport phenomena in classically chaotic systems.

1.2.2 Chaos in Quantum Mechanics

It is worth noting that one can also approach the problem of quantum chaos by asking what kinds of chaotic behaviors can be found in quantum systems. Part of the difficulty in carrying over classical chaos to quantum mechanics is that classical chaos is often defined in terms of the divergence of nearby trajectories, which do not have a straightforward quantum analog. If two nearly identical wave packets evolve, even in a nonintegrable system, the wave packets will remain close in the sense that their overlap integral is preserved under unitary time evolution; however, this is not a proper argument against chaos in quantum mechanics, as this argument applies also to the overlap integral of two classical phase space distributions evolving by the Liouville equation [Hilborn94]. A variation on this idea is to look at sensitivity to parameter perturbations, rather than perturbations to the quantum state, to uncover some quantum sensitive dependence. Because of the sensitivity to parameter perturbations of quantum states associated

with chaotic regions in phase space, the overlap of two initially identical wave packets evolving under slightly different Hamiltonians will drop exponentially under chaotic conditions, but will remain large in the stable case [Peres91b; Haake01; Gardiner97; Gardiner00]. This idea has also been extended to studying the sensitivity of wave-packet evolution under randomly perturbed Hamiltonians, which shows a marked difference between stable and chaotic conditions [Schack93; Schack94].

It is also possible to focus on the short-time quantum dynamics, where the behavior resembles that of classical chaos, as is apparent in the initial diffusive phase of the quantum kicked rotor [Chirikov87] shown in Fig. 1.5. Furthermore, initially localized wave packets can also show exponential instability for short times [Toda87; Fox94; Lan94], as expected for a similar classical distribution. Hence Chirikov [Chirikov92] has advanced the notion of *finite-time* quantum chaos. There are also examples of genuine chaos where quantum mechanics is involved. Quantum systems can give rise to chaotic behavior when coupled to a classical system, as is the case for example with two-level atoms in a cavity coupled to a classical field [Belobrov77; Milonni83; Fox90] or in a quantum-mechanical oscillator coupled to a classical oscillator [Cooper94]. It has even been argued that chaos is possible in a purely quantum-mechanical system obtained by quantizing a classical chaotic system, although not by the usual quantization procedure, and this "configurational chaos" requires that the canonical momenta be unbounded [Chirikov88; Weigert93; Peres96]. (Another proposal for a purely quantum chaotic system [Blümel94] seems suspect in that the apparatus itself must become exponentially more complicated as the evolution continues, and additionally shows sensitivity to perturbations of the system parameters rather than to perturbations of the quantum state [Schack95].)

Finally, we note that the concept of the trajectory is central to the de Broglie–Bohm formulation of quantum mechanics, so it is natural to look for chaotic behavior of these trajectories [Bohm93]. Interestingly, though, it has been found that the de Broglie–Bohm trajectories can be chaotic even for an integrable billiard [de Alcantara Bonfim98], so in a sense there is "too much" chaos in the de Broglie–Bohm picture, in contrast to the "not enough" chaos in standard quantum mechanics. It is not clear, however, that these chaotic trajectories have any mean-

ingful predictive power outside the statistical ensemble that reproduces the results of standard quantum mechanics.

1.2.3 Experiments in Quantum Chaos

By far the majority of progress in the field of quantum chaos has been theoretical, but now there has developed a large body of experiments to complement the theoretical advances. In this section we give a very brief and far from complete overview of experimental work in quantum chaos to illustrate the variety of systems in which the ideas of quantum chaos are important. An important first step towards experimental study in this area was taken with the work of Bayfield and Koch on the multiphoton ionization of hydrogen Rydberg atoms [Bayfield74]. A discrepancy between the measured ionization thresholds and the predictions of classical models provided the first experimental evidence of dynamical localization [Galvez88; Bayfield89; Koch95]. Subsequently, Rydberg atom ionization experiments have given rise to a variety of interesting phenomena [Blümel97], including scarring effects [Koch92; Koch95] and effects due to "metamorphoses" of classical resonances as the field strength is varied [Bayfield96]. The spectroscopy of atoms in external fields also provides a frequency-domain arena for tests of quantum chaos, including level statistics [Delande91; Delande01] and the influence of periodic orbits [Eichmann88; Main91; Gutzwiller90]. The statistics of resonances in atoms, molecules, and nuclei have also been shown to exhibit level-repulsion effects [Eckhardt88; Haake01].

As mentioned before, mesoscopic semiconductor structures provide an important arena for the study of quantum chaos [Stöckmann99]. Conductance measurements of semiconductor billiard structures show "universal conductance fluctuations" and weak localization effects with the application of strong magnetic fields [Marcus92; Stöckmann99]. The tunneling current through quantum-well heterostructures ("resonant tunneling diodes") can also be understood in terms of unstable periodic orbits in a chaotic regime [Fromhold94] and show effects due to scarring [Wilkinson96a]. Semiconductor antidot lattices provide a different setting for studying conductance fluctuations with applied magnetic fields [Weiss91; Weiss93], giving an experimental realization of the Lorentz gas [Stöckmann99]. Another related billiard-like system is the

"quantum corral" [Crommie95], where a scanning tunneling microscope (STM) can be used to move individual atoms on a surface to build a confining structure for electrons.

A different class of experiments explores the area of "wave chaos," exploiting the formal equivalence of various other wave equations to the Schrödinger equation under certain circumstances. Perhaps the most notable among these are the microwave-cavity billiard experiments [Stöckmann99], in which such topics as level statistics [Stöckmann90], scarring [Sridhar91], dynamical localization [Sirko00], chaos-assisted tunneling [Dembowski00], and a trace formula [Dembowski01] have been studied. This line of analysis has been extended to the study of deformed micro-disk cavity lasers, which act as open billiard systems in the optical domain [Gmachl98]. A similar realization of wave chaos occurs with the mechanical vibrations of aluminum blocks [Weaver89; Ellegaard95] or rigid plates [Neicu01; Stöckmann99], and billiard-type experiments can be carried out using surface waves [Lindelof86; Blümel92; Kudrolli01] or ultrasonic waves [Chinnery96] in fluids. Many of these billiard-type experiments are reviewed in [Stöckmann99]. Finally, the equivalence of the electromagnetic equation in the paraxial approximation with the Schrödinger equation can be exploited to create an optical realization of the kicked rotor [Fischer00; Rosen00].

Of course, the field of atom optics provides a clean and precise setting for experimental explorations of quantum chaos, including the dynamical localization effect that we have introduced, but we defer this discussion until Section 1.4.

1.2.4 On the "Usefulness" of Quantum Chaos

The field of quantum chaos is generally associated with fundamental interests in quantum mechanics, because of the initial motivation in this field to understand the interplay and correspondence of quantum and classical mechanics. However, it is worth pointing out that quantum chaos is also emerging as a field with important technological applications, and hence progress in this field is desirable also from an applied standpoint. One obvious area where these ideas will be important is in the semiconductor and microprocessor industries, where the nearly exponential increase in density of components will soon lead to sufficiently small devices that

quantum effects will be significant. Present devices are strongly coupled to the environment at normal operating temperatures, so that the electron coherence length is very short and thus quantum effects are only important at very low temperatures, as in the conductance fluctuation experiments mentioned above. But when quantum effects take over, the semiconductor devices will obviously not have the high degree of symmetry necessary for integrability, so the charge transport in these devices will fall in the regime of quantum chaos. Along these same lines, the future development and demonstration of quantum computers [Steane97] will require careful consideration of effects due to classical chaos to ensure proper operation [Georgeot00].

As we have already discussed, quantum chaos has been important in the understanding of atomic spectra. Quantum chaos has also been shown to be of importance in the dynamical manipulation of atoms by light [Robinson96]. However, there are many more applications of quantum chaos outside of quantum mechanics in other wave systems. For example, quantum-chaos effects are important in the understanding of underwater acoustics [Sundaram99b]. We have also already mentioned the applicability of quantum chaos to the understanding of the mode structure of microwave cavity devices and mechanical vibrations. In a similar optical analogy, weakly deformed micro-disk semiconductor lasers show large improvements in directionality and intensity over normal whispering-gallery mode lasers, which is an application of wave chaos in an open system [Gmachl98]. Finally, a fiber-optical switch for the communication industry has been proposed [Vorobeichik98], based on the ideas of chaos-assisted tunneling, which we study in Chapter 6. In fact, a company (OpTun Ltd.) has been founded to develop these ideas.

1.3 Decoherence

The lack of long-time chaotic behavior in quantum mechanics seems to bring up difficulties in how the theories of quantum and classical physics are related. Specifically, since quantum mechanics is believed to be the more universal theory, it should in some sense "contain" classical mechanics as a limiting case. This idea, first advanced by Bohr, is known as the *Correspondence Principle*, and showing how classical-quantum correspondence arises remains even now a controversial and challenging problem. But because quantum mechanics does not support chaotic

behavior in the sense of classical mechanics, it seems, oddly, that chaos cannot exist even in classical mechanics, if we are to believe in correspondence. In a simplistic view one might expect to recover classical mechanics by formally taking the limit $\hbar \to 0$ (of course, since Planck's constant $\hbar$ is indeed a constant, what we really mean is that we are taking the limit where the action of a system becomes arbitrarily large compared to $\hbar$). However, this limit is highly singular and not necessarily well-defined, as one can see from the form of the WKB wave function $\psi \sim \exp(iS(x)/\hbar)$ (where S is the action of the system) that applies in the "semiclassical" regime of small $\hbar$, which has an essential singularity at $\hbar = 0$.

One path to correspondence is suggested, for example, by the initially diffusive behavior in the kicked rotor that we noted above, which mimics the diffusion characteristic of classical chaos. It has been argued [Chirikov87; Cohen91; Delande01] that the "quantum break time" t_{B}, when the behavior crosses over from diffusive to localized, scales as $1/\hbar^2$, since in an energy-time uncertainty sense, this is the time required for the discrete spectrum to become "resolvable" by the system. Hence, it would seem that for macroscopic systems, the break time could become unobservably long because $\hbar$ would effectively be very small. However, there is a second time scale for quantum deviations from classical behavior, known as the "Ehrenfest time" t_{E}, which scales much more slowly, as $\log(1/\hbar)$. The existence of this time was pointed out originally by [Berman78] for a specific model, and this time scale was discussed by [Adachi88; Cohen91] in the context of the kicked rotor, by [Karkuszewski01] for another driven, one-dimensional system, and by [Zurek94] for general chaotic systems. We will discuss the origin of this time scale in more detail below. The slow scaling of this time has dire consequences for correspondence, for although this time scale diverges as $\hbar \to 0$, in physical reality $\hbar$ is always some nonzero value, and thus spanning 30 orders of magnitude in $\hbar$ from a manifestly quantum regime to a manifestly classical regime yields a relatively minor change in t_{E}. By this argument, then, we would predict absurdly short times for which quantum effects should set in for classically chaotic systems [Adachi89; Zurek95]. Since this obviously violates common experience in the macroscopic world, there is clearly a need to resolve this discrepancy between the quantum and classical pictures.

One solution to this problem is embodied in the theory of *decoherence*. The key idea here is that macroscopic objects are in general not very well isolated from their "environment," which could, for example, include the internal (thermal) degrees of freedom or the ambient photons scattering off the object. Decoherence provides a mechanism by which the quantum coherence effects that suppress chaos can themselves be suppressed. Thus, even though it seems clear that classical behavior does not, in general, arise as a limit of the Schrödinger-equation description, it can arise as a limit of an "open" quantum description that takes into account the external influences on the system [Joos85].

Broadly speaking, there are two "roles" of decoherence in explaining classical behavior as a consequence of quantum mechanics. The first is the suppression of quantum superposition states at the classical level, which addresses the famous Schrödinger cat paradox and is intimately related to the quantum-measurement problem [Wheeler93; Giulini92]. The second role of decoherence is in ensuring classical behavior in the dynamical evolution of a system. These two roles are, of course, closely related, but we will discuss them separately according to how they are applied in explaining classicality.

1.3.1 Suppression of Quantum Superposition

In Schrödinger dynamics, the state of the system is described by the wave function or state vector. For open systems, though, a more natural representation of the system is in terms of the *density operator*. For a state $|\psi\rangle$, the density operator is defined as

$$\hat{\rho} := |\psi\rangle\langle\psi| \quad . \tag{1.14}$$

In this case the *density matrix* (the representation of the density operator in a particular basis) is highly redundant, because if the state vector has n components in some finite basis, the density matrix has n^2 components, but does not contain additional information. However, the density matrix has the advantage that it can be generalized to an ensemble in a straightforward way simply by averaging over the members $|\psi_j\rangle$ of the (usually large) ensemble,

$$\hat{\rho} := \frac{1}{N}\sum_j |\psi_j\rangle\langle\psi_j| \quad . \tag{1.15}$$

A state corresponding to a wave vector as in (1.14) is referred to as a *pure state*, whereas an ensemble average as in (1.15) is a *mixed state*. The diagonal elements $\rho_{\alpha\alpha} = \langle\alpha|\hat{\rho}|\alpha\rangle$ of the density matrix are the *populations*, as they represent the probability of occupying the state $|\alpha\rangle$. The off-diagonal elements $\rho_{\alpha\beta} = \langle\alpha|\hat{\rho}|\beta\rangle$ ($\alpha \neq \beta$) contain the relative-phase information of the state, and are referred to as *coherences*. The important feature of the coherences to note here is that they have their maximum magnitude for a pure state. In a mixed state, if the phases of the various components are not aligned, the magnitudes of the coherences are reduced, falling to zero for a completely uncorrelated ensemble. Notice that because the coherences represent the potential for interference effects, they are in effect the "nonclassical" part of the density matrix. It is only the populations that have a sensible interpretation as classical probabilities.

The treatment of a system interacting with its environment begins typically by identifying the degrees of freedom associated with the "system" of interest and the "reservoir" which represents the environment. The combined system is then represented by the density operator $\hat{\rho}_{\mathrm{S+R}}$, and we assume that this combined system is now "closed" in the sense that there are no interactions with other systems that are not already described by this density operator. In a closed system, the density operator evolves according to the Schrödinger-von Neumann equation

$$\partial_t \hat{\rho} = -\frac{i}{\hbar}[H, \hat{\rho}] \ , \tag{1.16}$$

which gives the same evolution as the Schrödinger equation for the state vector. Hence a pure state, treated as a closed system, will evolve into a pure state as a consequence of the "unitarity" of the evolution equation. However, since we are generally interested in the system, which may have only a few degrees of freedom, we would like to ignore the information associated with the reservoir, which typically has many more degrees of freedom than we could possible monitor. One approach along these lines is suggested by the form for expectation values of operators in terms of the trace over the density matrix:

$$\langle\hat{A}\rangle = \mathrm{Tr}[\hat{A}\hat{\rho}] \ . \tag{1.17}$$

The average over the reservoir is then given by a partial trace taken over the reservoir degrees of

freedom, resulting in a "reduced" density operator that describes only the state of the system:

$$\hat{\rho}_{\rm S} = {\rm Tr}_{\rm R}[\hat{\rho}_{\rm S+R}] \ . \tag{1.18}$$

In general, the evolution of $\hat{\rho}_{\rm S}$ depends on its history, but in the case where the reservoir is large, it should decorrelate rapidly, and so a Markovian approximation is justified. In this case it is possible to derive a *master equation* for the evolution of $\hat{\rho}_{\rm S}$ [Cohen-Tannoudji92], which is similar to the unitary evolution equation (1.16) but with extra nonunitary terms describing the exchange of energy with the environment (dissipation or relaxation) and the redistribution of populations due to fluctuations in the environment (diffusion) [Zurek91; Zurek94]. In terms of the density matrix, these new terms cause the evolution of a pure quantum state into a mixed quantum state, since the diffusion terms cause the coherences to be damped away [Zurek91; Cohen-Tannoudji92]. Although the interferences that were initially in the system still exist, they are moved out of the system and into the reservoir as the system and reservoir become entangled through their interaction [Joos85].

The idea of decoherence, in its simplest form, is that the interaction with the environment can suppress the quantum coherences on a time scale that is many orders of magnitude shorter than the time scale associated with relaxation [Zurek91]. So, while the environment has a negligible impact on the "classical aspects" of the system, the coherences can be suppressed effectively instantaneously in a macroscopic system. The resulting diagonal density matrix can then be interpreted as a classical probability distribution.

The question that now arises is why the density operator should become diagonal in a particular basis and not some other. The answer depends, of course, on the nature of the environmental interaction. It has been argued [Zurek81; Zurek82; Paz93] that the environment naturally selects a preferred ("pointer") basis, which consists of those states that are minimally affected by the environment (i.e., they become minimally entangled with the environment). These states are, in a sense, "robust" to the decoherence. This principle of "environment-induced superselection" [Paz93] highlights the relation of decoherence to the measurement of a quantum system. Such a measurement necessarily entails an interaction with the environment,

namely the measuring apparatus [Paz99]. The nature of the interaction is tailored to the measurement of some observable, and the minimally coupled states are determined by a combination of the system Hamiltonian and the interaction Hamiltonian for the environmental coupling. A measurement may require a strong interaction that dominates the system Hamiltonian, so that the pointer states are the eigenvalues of the interaction Hamiltonian, leading naturally to the idea that measurement "collapses" the system into an eigenstate of the operator corresponding to the measured observable. The naturally selected states have also been demonstrated, for example, to be localized states in phase space in the case of an environmental coupling (of intermediate strength) to the position of a particle [Paz93], coherent states for the weakly coupled harmonic oscillator [Zurek93], and energy eigenstates in the regime of weak coupling to the environment, where the system Hamiltonian is dominant [Paz99]. Beyond the reduction to a classical mixture, decoherence addresses the issue of how a quantum system is forced into a definite state by the measurement interaction (notice that the only diagonal, pure-state density operators correspond to the basis states). The "measurement" is made by the environment, in that the entanglement with the environment transfers information to the environmental degrees of freedom. The statistical mixture that we are left with in the master-equation description is a reflection of our ignorance of the state of the environment, which in a macroscopic system is too complicated to keep track of even in principle. Since the outcome of the measurement is intimately tied to the immensely complicated environment, the measurement appears as a "random" collapse of the state vector. Thus, decoherence attempts to bring the measurement process back within the unitary evolution framework of quantum mechanics, without appealing to an extraneous notion of wave-function collapse, as in the orthodox interpretation of quantum mechanics [Joos85; Zurek91].

1.3.2 Classical Chaotic Evolution

So far, we have seen that the interaction with the environment can take a state with quantum features and convert it into a state that is sensible in a classical description. More important for the correspondence principle in dynamical systems, however, is to understand how decoherence can cause the *evolution* of a quantum system (which we have seen is particularly problematic in

nonintegrable systems) to cross over to classical behavior.

One important tool for this discussion is the Wigner function (or distribution), which facilitates the description of quantum dynamics in phase space. The Wigner function is defined in terms of the density matrix as [Wigner32; Schleich01]

$$W(x,p) := \frac{1}{\pi\hbar}\int_{-\infty}^{\infty} dx' e^{2ipx'/\hbar}\langle x-x'|\hat{\rho}|x+x'\rangle \quad . \tag{1.19}$$

The Wigner function is not the only quantum phase-space distribution [Hillery84], but it has several features that make it preferable to other distributions. Each marginal distribution of the Wigner function, where one of the variables is integrated out, results in the probability distribution corresponding to the other variable. The Wigner function itself, however, is not a joint probability distribution, since it can take on negative values, which represent the interferences or coherences of the quantum state. The evolution of the Wigner function (for one degree of freedom) can be expressed in terms of the Moyal bracket of the Hamiltonian and the Wigner function [Moyal49; Reichl92; Shiokawa95],

$$\begin{aligned} \partial_t W(x,p) &= \{H,W\}_{\rm M} \\ &:= -\frac{2}{\hbar}H(x,p)\sin\left[\frac{\hbar}{2}\left(\overleftarrow{\partial_p}\overrightarrow{\partial_x} - \overleftarrow{\partial_x}\overrightarrow{\partial_p}\right)\right]W(x,p) \quad , \end{aligned} \tag{1.20}$$

where the arrows on the derivative operators indicate the direction of operation. For a particle Hamiltonian in "standard form," $H = p^2/(2m) + V(x)$, the Moyal bracket can be written as the Poisson bracket plus quantum "correction" terms,

$$\partial_t W = \{H,W\}_{\rm P} + \sum_{n=1}^{\infty}\frac{(-1)^n\hbar^{2n}}{2^{2n}(2n+1)!}(\partial_x^{2n+1}V)(\partial_p^{2n+1}W) \quad . \tag{1.21}$$

This equation is especially suitable for comparing the quantum evolution with the evolution of a classical ("Liouville") distribution $\rho_{\rm L}$,

$$\partial_t\rho_{\rm L}(x,p) = \{H,\rho_{\rm L}\}_{\rm P} \quad , \tag{1.22}$$

which is described only by the Poisson bracket. Notice that formally setting $\hbar = 0$ in (1.21) recovers the Liouville evolution (1.22), so that correspondence seems easy in this formulation;

however, it must be emphasized that taking the limit $\hbar \to 0$ for a quantum system is not trivial and may not be well defined without the assistance of external degrees of freedom.

It is immediately clear from the form of the Moyal bracket (1.21) that quantum-classical correspondence is particularly simple for "linear" systems, such as a free particle or a harmonic oscillator, because the quantum-correction terms vanish, yielding identical quantum and classical evolution equations. This point was recognized early on by Schrödinger, when he constructed the coherent states of the harmonic oscillator that mimic the classical oscillating trajectories [Schrödinger26]. Hence, all that is needed for correspondence in these systems is the action of decoherence for a mere instant (say, a single measurement), after which the quantum evolution preserves the classicality of the state. In the more general and challenging case, the nonlinearities of the system dynamically generate quantum interferences in the course of evolution [Habib98b]. The quantum terms cause the evolution to be unitary (notice that the classical evolution, even for a closed system, is manifestly nonunitary [Habib00]), and thus it is these quantum terms that are responsible for the suppression of classical chaos. (Note that this is a much more meaningful way to treat the absence of chaos in quantum mechanics than simply appealing to the linearity of the Schrödinger equation.) The picture of quantum-classical divergence according to [Zurek94] is that because of the exponential stretching of a Liouville distribution under chaotic evolution, the distribution develops fine structure on a very short time scale. Since the quantum-correction terms involve derivatives of the Wigner function, they will be unimportant for an initially smooth distribution, but will quickly become important as fine structure develops due to the classical part of the evolution. From this argument, we expect the $\log(1/\hbar)$ breakdown time that we mentioned earlier as a consequence of exponential chaotic divergence. To achieve correspondence in the nonlinear regime, a single measurement at a single time during the evolution is insufficient to cause agreement between classical and quantum. For example, in the case of dynamical localization it is insufficient to decohere the system after the quantum break time, because although such an action would temporarily restore diffusive behavior, it would already be "too late," as the subsequent evolution could never catch up to the corresponding classical, continuously diffusing evolution. Rather, it is impor-

tant to have continuous decoherence, which would effectively broaden the spectral components of the evolution and never allow the discreteness of the spectrum to become manifest. In the picture of [Zurek94], the interaction with the environment results in additional diffusive terms in the evolution equation (corresponding to the diffusion terms in the master equation for the density-matrix evolution) that tend to smooth the Wigner function. The resulting evolution is a balance between the usual evolution, which wants to generate fine structure, and the decoherence, which wants to destroy the same fine structure. For sufficiently strong noise, the fine structure can be tempered to the point where the quantum corrections remain unimportant, and the evolution is the same as that of the classical system subject to the same diffusive interaction. In the semiclassical limit, only a very small amount of noise is required to keep the quantum corrections under control (diffusion is only necessary on the scale of an $\hbar$ cell in phase space), so that the effect on the classical chaos is effectively negligible. This argument gives a nice picture of how decoherence can induce classical evolution, but we should note that there are some subtleties that may still need to be addressed for certain systems, including the kicked rotor [Habib00].

In studying the decoherence due to environmental interaction, it is possible to use an approach based on the master equation [Brun96; Gong99; Bhattacharya00] that models all of the effects due to the environment, or a simplified approach that employs an external noise source [Ott84; Adachi88; Scharf94]. The latter approach is justified because the noise-induced diffusion (not dissipation) is mostly responsible for the decoherence [Zurek94; Helmkamp96]. Furthermore, there are several levels at which correspondence has been examined in various theoretical studies. The most qualitative is the removal of nonclassical features by decoherence, including the destruction of scarred states [Scharf94] and the restoration of the irreversibility that is so conspicuously absent in unitary quantum evolution [Shiokawa95]. At the next level is the quantitative agreement of quantum and classical expectation values [Ott84; Gong99; Bhattacharya01]. Although such quantitative agreement is important, the expectation values carry only a small amount of information about the system, which motivates the study of correspondence at the level of ensembles and distribution functions [Adachi89; Habib98b]. Even

here, though, it is possible to have agreement at the ensemble level even in a quantum regime [Gong99], where it may still not be possible to associate classical trajectories with quantum evolution. Hence the strongest form of correspondence is obtained in a quantum trajectory approach, where a decoherence-influenced wave packet traces out a chaotic trajectory with the same properties as a corresponding classical trajectory (with noise added to the classical system to account for the "direct" contribution of the decoherence) [Spiller94; Brun96; Bhattacharya00; Scott01].

It has been argued that an appeal to the influence of the environment is not necessary for correspondence, but rather a coarse-graining, as for example manifested in the Husimi distribution [Hillery84], can serve to remove the nonclassical structure of the Wigner distribution [Casati95]. However, as pointed out in [Habib98b], such an approach will not in general be successful because this coarse graining hides the nonclassical features in an essentially trivial way (because it can be reversed); it does not change the dynamical evolution of the quantum system, which as we have seen is certainly necessary for correspondence; and the coarse graining forbids correspondence at the trajectory level, which is in a sense the most impressive form of correspondence. The importance of environmental noise in explaining chaos is then somewhat ironic. Classical chaos is usually understood as arising solely from the system itself and not from an external noisy source, as we have pointed out in Section 1.1. At a deeper level, though, a certain amount of noise is necessary to obtain chaotic behavior from quantum mechanics. But because this noise level can be exceedingly small on macroscopic scales, the chaotic instability arises operationally from the "classical" dynamics rather than the perturbative noise.

1.3.3 Experiments on Decoherence

Despite the vast body of theoretical work on decoherence, there have been relatively few experiments dealing directly with the effects of decoherence on quantum systems. The situation is beginning to change now, though, due to the necessity of combating decoherence in systems where quantum coherence is very important, such as in quantum computers [Steane97]. In linear systems, there have been several impressive and clean experiments. The most funda-

mental linear quantum problem, the two-slit experiment, has been realized as an atom interferometer, where light scattered by the atoms serves as a decohering measurement [Chapman95; Kokorowski01]. Decoherence has also been studied in an entangled Rydberg atom/microwave cavity system [Brune96], where the cavity acts as a measuring device for the internal atomic state. The decoherence of a superposition of motional states has also been studied in an ion trap [Myatt00; Turchette00].

The first experimental studies in decoherence actually began with nonintegrable systems, where the effects of noise on the ionization of driven hydrogen [Bayfield91; Sirko93; Koch95; Sirko96] and rubidium [Blümel89; Arndt91; Blümel91; Benson95] Rydberg atoms were studied. Especially relevant to the work on correspondence that we discuss in Chapter 4 are Refs. [Bayfield91; Sirko93; Koch95], where noise added to the microwave driving of the Rydberg atoms led to improved agreement with classical predictions of ionization thresholds (which is an agreement at the expectation-value level, in contrast to the distribution correspondence that we present in Chapter 4). There has also been some work investigating the effects of temperature on conductance fluctuations in mesoscopic semiconductor quantum dots [Clarke95; Huibers98]. Optical-analog experiments open up the possibility for decoherence experiments in wave-chaos systems, where perturbations to diffraction-grating positions in an optical kicked-rotor realization led to destruction of dynamical localization [Fischer00; Rosen00]. Again, atom optics has contributed several experiments to this area, the discussion of which we defer until the next section.

1.4 Atom Optics

The field of *atom optics* is generally concerned with the manipulation of atoms using electromagnetic fields or material objects. In a sense, this field is the dual of traditional optics, where matter is used to manipulate electromagnetic (optical) fields. By far the majority of work in this field involves the optical manipulation of atoms, which is the case in this dissertation, although notable exceptions include the trapping of ions by electric fields [King99], the trapping of neutral atoms in static magnetic traps [Migdall85], the reflection of atoms by the Casimir–van der

Waals potential [Shimizu01], and the diffraction of atoms by lithographically fabricated gratings [Keith91]. The important concept in the optical manipulation of atoms is that light carries momentum. The momentum carried by photons is ordinarily very small, and macroscopic objects are generally immune to optical momentum effects. However, the momentum transferred to an atom when it scatters photons can have a very significant effect on its motion. Although the deflection of atoms by light ("radiation pressure") dates back to 1933 [Frisch33], it was not until the advent of lasers that much progress was made in this field. Subsequently the cooling of trapped ions using laser light was proposed [Hänsch75; Wineland75] and demonstrated soon thereafter [Wineland78; Neuhauser78]. The development of trapping and cooling of neutral atoms introduced more difficulties, though, because the optical forces are so weak compared to the electric-field forces used in ion traps, and so thermal atoms from an atomic beam were very difficult to trap. But the slowing of a thermal beam of atoms [Phillips82] and the subsequent demonstration of laser cooling of neutral atoms in three dimensions (using "optical molasses," where laser light acts as an effective damping medium for the atoms) [Chu85] led to magnetic [Migdall85] and optical [Chu86] traps for atoms.

It was, however, the addition of a magnetic field to optical molasses that revolutionized atomic physics. This idea, due to Jean Dalibard [Chu98], resulted in the efficient cooling and trapping of atoms from an atomic beam [Raab87] in a device now known as the *magneto-optic trap* (MOT). The MOT uses optical molasses to cool atoms, while simultaneously taking advantage of the Zeeman shift of the atomic energy levels in a magnetic field to introduce a spatial dependence on the radiation pressure and hence confine the atoms to the center of the trap. The MOT was considerably simplified when it was demonstrated that atoms could also be trapped directly from an ambient atomic vapor [Monroe90], and it is now relatively simple to construct a very basic MOT [Wieman95]. The MOT is now a true workhorse in atomic physics, as it provides a convenient, cold, localized, and well-controlled sample of atoms that can be used as the starting point for a wide range of experiments [Adams97], including Bose-Einstein condensation [Anderson95; Bradley95; Davis95], atom interferometry [Kasevich91], cold collisions and photoassociation spectroscopy [Gardner95], electric dipole moment searches [Bijlsma94],

precision atomic clocks [Gibble93], and atom lithography [Timp92; McClelland93]. Indeed, all the experiments that we describe in this dissertation are performed with a cesium MOT loaded from atomic vapor, much like the setup in [Monroe90], as discussed further in Chapter 3. For some of the experiments that we will discuss, much more elaborate preparation of the atoms is necessary after the initial trapping and cooling of the atoms, as described in Chapter 5.

1.4.1 The Dipole Force and Optical Lattices

The forces used in a MOT are due to the absorption and spontaneous emission of light. Because the direction of a spontaneously emitted photon is random, this force is incoherent and results in the diffusion of momentum on the scale of the atomic recoil momentum due to a single photon scattering event (the "photon-recoil momentum"). Although this force is useful for the collection and preparation of atoms, the subsequent manipulation of atoms is greatly facilitated by the use of the *dipole force*, which does not involve dissipation or diffusion, and is thus a coherent interaction. The dipole force is a result of the interaction of an optical field and the atomic dipole moment induced by the field. The dipole interaction energy has the form $-\mathbf{d}\cdot\mathbf{E}$, where $\mathbf{d}$ is the atomic dipole moment and $\mathbf{E}$ is the electric field. Since the induced dipole moment is proportional to the applied field, the optical potential is proportional to the field intensity, and thus the dipole force is proportional to the gradient of the field intensity. In a photon picture, this force arises as a consequence of stimulated scattering of photons by the atom, where the redirection of a scattered photon results in a corresponding "recoil" by the atom. This effect is also known as the *ac Stark shift* or *light shift* of the atomic energy, and was first observed by Cohen-Tannoudji [Cohen-Tannoudji98]. Thus, it is possible to create potentials to influence atomic motion by appropriately tailoring an optical-field profile. Also, if the optical field is tuned sufficiently far from the nearest atomic resonance, the interaction will be dominated by the dipole force, and spontaneous forces will be negligible.

One particular configuration in which the dipole force is important is the *optical lattice*, which is a periodic intensity pattern formed by the interference of multiple beams. Although there are many different possible configurations of optical lattices [Jessen96], the one

that plays a central role in the experiments in this work is the simplest possible lattice, a standing wave of light, which is a one-dimensional, linearly polarized optical lattice. We discuss this configuration in detail in Chapter 2, but the basic result is that the atomic motion in such a standing wave is that of a quantum pendulum (without periodic boundary conditions). This system can then be viewed as an ideal one-dimensional crystal with long coherence times [Niu96; Madison98a; Fischer01b], leading to interesting and clean studies of effects in condensed-matter physics [Wilkinson96b; Dahan96; Fischer98; Madison98b; Madison99]. Viewed also as a one-dimensional dynamical system, this system gives rise to interesting tunneling effects [Morrow96; Bharucha97a; Madison97], including non-exponential decay [Wilkinson97] and the quantum Zeno and anti-Zeno effects [Fischer01a].

1.4.2 Atom Optics and Quantum Chaos

The fields of quantum chaos and atom optics became "entangled" with the proposal by Graham, Schlautmann, and Zoller [Graham92] to observe dynamical localization in the deflection of an atomic beam crossing through a phase-modulated optical lattice. It was realized here in the group of Mark Raizen that the beam setup could be "collapsed" and performed with cold atoms prepared by a MOT and exposed to a modulated optical lattice in place. An apparatus using trapped sodium atoms was constructed [Robinson95b; Bharucha97b], and the manifestations of dynamical localization [Moore94] and islands of stability (and other features in the transition from classical stability to chaos) in phase space [Robinson95a] were studied in the phase-modulated lattice. (It was also in these experiments that the "ballistic-expansion imaging method" of measuring atomic momentum distributions was first employed. In this technique the atoms expand freely after the lattice interaction until they have expanded far beyond the initial MOT size, then they are frozen in place by optical molasses, and the distribution is photographed by a CCD camera.) In the phase-modulated system, the theoretical understanding of dynamical localization came about through an approximate mapping onto the kicked-rotor problem, and this system was soon also directly realized [Moore95]. In these experiments, the dynamical evolution leading to localization was studied, along with the "quantum resonance" phenomenon, which is expected to give rise to ballistic transport but was manifested as a late-

time Gaussian distribution. The atomic dynamics in an amplitude-modulated standing wave, which is the same system that we use in Chapter 6 to study chaos-assisted tunneling, were also studied using this apparatus to address the necessity of considering quantum chaos in analyzing a system as simple as atoms crossing transversely through an unmodulated optical lattice [Robinson96]. The work in this first-generation sodium apparatus is discussed in more detail in [Bharucha99], as well as in two dissertations [Robinson95b; Bharucha97b].

The next natural direction of the quantum-chaos experiments was to examine the effects of decoherence, now that the quantum suppression of chaos had been observed. As these experiments involve transport to higher momenta than in the localized case, the sodium-based experiment was not suitable to carry out these studies [Robinson95b]. To address these problems with the "momentum boundary" [Klappauf99], we constructed a second-generation apparatus based on trapped cesium, which due to the longer wavelength of the atomic resonance and larger atomic mass effectively yields a better fidelity to the δ-kicked rotor over a wider momentum range (see Section 4.4.4 for details). The quantum-chaos experiments carried out on this new apparatus are reviewed in this dissertation as well as in Bruce Klappauf's dissertation [Klappauf98c], and meanwhile the sodium apparatus was put to good use in the tunneling and solid-state experimental efforts described in the previous section. The destruction of localization by amplitude noise in the kicks as well as dissipation due to the presence of a weak optical molasses were observed in this experiment [Klappauf98b], where it was found that late-time energy diffusion was increased, and the momentum distributions made a transition from the localized exponential profile to a classical-like Gaussian profile. Around the same time, the increased energy growth due to spontaneous emission induced by the optical lattice itself was observed by the group of Nelson Christensen [Ammann98], but it should be noted that there may be some difficulties in interpreting the results of this latter experiment due to the influences of the classical momentum boundary and the stochastic dipole force [Habib98a]. We subsequently extended this initial work on decoherence and showed that quantitative quantum-classical correspondence at the level of expectation values and momentum distributions could be achieved with a sufficient amount of amplitude noise, even in a manifestly quantum regime [Steck00; Milner00].

This work on decoherence and correspondence in the kicked rotor is discussed in much more detail in Chapter 4.

There have also been several other interesting avenues of experiments on quantum chaos and quantum transport in atom optics. We revisited the quantum resonance phenomenon using the cesium apparatus, and due to much improved signal resolution and noise levels over the original study of [Moore95], we were able to resolve the ballistic component of the motion [Oskay00]. There have also been related studies by the group of Keith Burnett [Oberthaler99; Godun00] on the kicked rotor near a quantum resonance but modified by a constant acceleration. Ballistic transport was likewise observed in these experiments, but the transport could be made directional (asymmetric) due to the influence of the acceleration. Continuing in the vein of global quantum nonintegrable transport, the suppression of diffusion by classical cantori was studied by the Christensen group [Vant99], the effects of quasiperiodic kicking were studied by a group at the Université des Sciences et Technologies de Lille [Ringot00], and we provided experimental evidence for a universal theory of quantum diffusion by Jianxin Zhong, Qian Niu, Roberto Diener, and others [Zhong01]. More recently, work in this area has moved towards the study of mixed phase space using localized initial conditions. In this context we have observed chaos-assisted dynamical tunneling [Steck01], and a collaboration of researchers at NIST-Gaithersburg under the direction of William Phillips and Steven Rolston and researchers at the University of Queensland under the direction of Gerard Milburn, Halina Rubinsztein-Dunlop, and Norman Heckenberg have also observed dynamical tunneling in a similar system (using a Bose-Einstein condensate) but in a more manifestly quantum and strongly coupled regime [Hensinger01] (some earlier work of the Queensland group is discussed in [Hensinger00]). Our work on chaos-assisted tunneling is described in detail in Chapter 6. Finally, we have performed experiments on a modified version of the kicked-rotor system that leads to spatial localization of the atoms, with applications to atom lithography. The results of this work will be presented in future publications [Oskay01a; Oskay01b].